

RESEARCH ARTICLE

Mitochondrial fission is required for cardiomyocyte hypertrophy mediated by a Ca^{2+} -calcineurin signaling pathway

Christian Pennanen^{1,2}, Valentina Parra^{1,2,3}, Camila López-Crisosto^{1,2}, Pablo E. Morales^{1,2}, Andrea del Campo^{1,2}, Tomás Gutierrez^{1,2}, Pablo Rivera-Mejías^{1,2}, Jovan Kuzmivic^{1,2}, Mario Chiong^{1,2}, Antonio Zorzano^{4,5,6}, Beverly A. Rothermel^{3,*} and Sergio Lavandero^{1,2,3,*}

ABSTRACT

Cardiomyocyte hypertrophy has been associated with diminished mitochondrial metabolism. Mitochondria are crucial organelles for the production of ATP, and their morphology and function are regulated by the dynamic processes of fusion and fission. The relationship between mitochondrial dynamics and cardiomyocyte hypertrophy is still poorly understood. Here, we show that treatment of cultured neonatal rat cardiomyocytes with the hypertrophic agonist norepinephrine promotes mitochondrial fission (characterized by a decrease in mitochondrial mean volume and an increase in the relative number of mitochondria per cell) and a decrease in mitochondrial function. We demonstrate that norepinephrine acts through α_1 -adrenergic receptors to increase cytoplasmic Ca^{2+} , activating calcineurin and promoting migration of the fission protein Drp1 (encoded by *Dnm1*) to mitochondria. Dominant-negative Drp1 (K38A) not only prevented mitochondrial fission, it also blocked hypertrophic growth of cardiomyocytes in response to norepinephrine. Remarkably, an antisense adenovirus against the fusion protein Mfn2 (*AsMfn2*) was sufficient to increase mitochondrial fission and stimulate a hypertrophic response without agonist treatment. Collectively, these results demonstrate the importance of mitochondrial dynamics in the development of cardiomyocyte hypertrophy and metabolic remodeling.

KEY WORDS: Calcineurin, Drp1, Cardiac hypertrophy, Metabolism, Mitochondrial fission, Norepinephrine

INTRODUCTION

Cardiac hypertrophy is an adaptive compensatory cellular mechanism that is activated in response to a wide variety of stimuli, including hemodynamic overload, neurohormonal activation, ischemia or intrinsic defects in genes encoding cardiac structural proteins (Marian and Roberts, 1995; Frey et al., 2004; Barry et al., 2008). At the cellular level, cardiomyocytes undergo

several morphological and functional changes characterized by increases in cell size, contractile protein content and sarcomere assembly, in addition to changes in gene expression and mechanical properties, culminating in an increase in heart size (Ruwhof and van der Laarse, 2000; Ahuja et al., 2007). Initially, cardiac hypertrophy can be beneficial because it improves myocardial function; however, prolonged biomechanical stimulation leads to pathological cardiomyocyte growth characterized by alterations in the extracellular matrix, loss of adrenergic responsiveness, changes in metabolism, and altered expression of some contractile proteins (Diwan and Dorn, 2007; Bernardo et al., 2010). Together, these changes can lead to cell death and irreversible structural cardiac remodeling associated with progressive ventricular dilatation and heart failure (Diwan and Dorn, 2007; Bernardo et al., 2010).

The adrenergic system plays a key role in cardiac remodeling (Barki-Harrington et al., 2004). Norepinephrine triggers cardiomyocyte hypertrophy through the activation of specific signaling pathways, including the Ca^{2+} -activated protein phosphatase calcineurin (Taigen et al., 2000; Shibasaki et al., 2002; Wilkins and Molkenin, 2004; Heineke and Molkenin, 2006). Molkenin et al. demonstrated that transgenic mice with cardiac-specific expression of a constitutively active form of calcineurin developed cardiac hypertrophy that quickly progressed to a dilated cardiomyopathy with signs of interstitial fibrosis and congestive heart failure (Molkenin et al., 1998).

Mitochondrial function is essential for proper heart function. Cardiomyocytes need a large and constant supply of energy in order to accomplish an array of specialized and complex cellular processes including continuous repetitive contraction, maintenance of Ca^{2+} homeostasis and coordinated function of diverse ion transporters (Huss and Kelly, 2005). Given the high density of mitochondria in cardiomyocytes and the absolute dependence on mitochondrial oxidative phosphorylation to generate ATP for cardiac contraction, it is not surprising that pathological alterations in this tissue are often associated with changes in mitochondrial metabolism or function (Kuzmivic et al., 2011). In advanced pathological hypertrophy, numerous changes in mitochondrial metabolism have been reported, including changes in substrate utilization, dysfunction of the electron transport chain and decreased capacity for ATP synthesis; resulting in a general deterioration of the cardiac metabolic function (Huss and Kelly, 2005; Neubauer, 2007). Furthermore, several studies have shown that mitochondrial disorders often present themselves as cardiomyopathies. For example, mutations that decrease mitochondrial oxidative phosphorylation or alter the activity of proteins involved in the transport of mitochondrial substrates (such as adenine

¹Advanced Center for Chronic Diseases (ACCDiS), Universidad de Chile, Santiago 8380492, Chile. ²Centro Estudios Moleculares de la Celula, Facultad Ciencias Químicas y Farmacéuticas & Facultad Medicina, Universidad de Chile, Santiago 8380492, Chile. ³Department of Internal Medicine (Cardiology Division), University of Texas Southwestern Medical Center, Dallas, TX 75235, USA.

⁴Institute for Research in Biomedicine (IRB), 08028 Barcelona, Spain.

⁵Departamento de Bioquímica i Biología molecular, Facultat de Biologia, Universitat de Barcelona, Barcelona, Spain. ⁶CIBER de Diabetes y Enfermedades Metabólicas Asociadas (CIBERDEM), Instituto de Salud Carlos III, Spain.

*Authors for correspondence (Beverly.Rothermel@UTSouthwestern.edu; slavander@uchile.cl)

nucleotide and fatty acid transporter proteins), can cause cardiac hypertrophy, as can the depletion of mitochondrial DNA itself (Buchwald et al., 1990; Graham et al., 1997; Stojanovski et al., 2004).

Mitochondria form highly dynamic networks, whose structure and distribution depend on the balance between the opposing processes of mitochondrial fission and fusion (Bereiter-Hahn and Vöth, 1994; Okamoto and Shaw, 2005; Chan, 2006). In mammalian cells, the main regulators of mitochondrial fusion are the dynamin-related GTPases mitofusin (Mfn) 1 and 2 and optic atrophy protein 1 (OPA1) (Chen et al., 2003; Ishihara et al., 2006; Song et al., 2009), whereas the mitochondrial fission 1 protein (Fis1) and the dynamin related protein-1 (Drp1, encoded by *Dnm1l*) control the mitochondrial fission process (Yoon et al., 2003; Jofuku et al., 2005). A continuous balance in mitochondrial dynamics is crucial for maintaining proper mitochondrial function. Furthermore, alterations in mitochondrial fission or fusion proteins are directly associated with mitochondrial dysfunction (Chen et al., 2005; Pich et al., 2005; Benard et al., 2007; Parone et al., 2008).

In the adult cardiac muscle, mitochondria are arranged in a longitudinal fashion, tightly packed between myofibrils, thus preventing the free movement of mitochondria through the cytosol (Vendelin et al., 2005; Beraud et al., 2009). In electron micrographs of normal heart tissue, intermyofibrillar mitochondria are often observed spanning a single sarcomere from Z-band to Z-band, suggesting that mitochondrial dynamics are under strict topological constraints. Indeed, the heart contains higher levels than other tissues of many of the proteins involved in the regulation of mitochondrial dynamics, and alterations in both fusion and fission processes have been associated with several pathological heart conditions (Kanzaki et al., 2010; Ong et al., 2010). For example, increased mitochondrial fission has been documented in models of ischemia–reperfusion and pharmacological inhibition of the mitochondrial fission protein Drp1 has been shown to reduce infarct size in mice subjected to coronary artery occlusion and reperfusion (Ong et al., 2010). Moreover, other studies using the α -adrenergic agonist phenylephrine to induce hypertrophy have demonstrated a decrease in mRNA levels of the mitochondrial fusion protein Mfn2 (Fang et al., 2007). In models of angiotensin-II-induced cardiac hypertrophy, pretreatment of cardiomyocytes with an adenovirus encoding *Mfn2*, increased Mfn2 expression and subsequently attenuated the hypertrophic response (Yu et al., 2011).

Taken as a whole, the clinical and experimental evidence point to an important role for mitochondrial dynamics in the development of cardiac hypertrophy. Nevertheless, how mitochondrial morphology and specific mitochondrial fusion and fission events affect the development of cardiomyocyte hypertrophy is still unclear. The aim of this study was to use a controlled *in vitro* system to test the relationship between mitochondrial dynamics and cardiomyocyte hypertrophy. Mitochondrial morphology and function were studied and manipulated in cultured neonatal rat cardiomyocytes treated with norepinephrine to model an adrenergic hypertrophic stimulus and ascertain the contribution of mitochondrial dynamics to the hypertrophic response.

RESULTS

Norepinephrine induces mitochondrial fission in cultured cardiomyocytes

To characterize the morphological changes of the mitochondrial network during hypertrophic cardiomyocyte growth triggered

by catecholamines, cultured cardiomyocytes were treated with norepinephrine (10 μ M, 0–48 h) and stained with the mitochondrial-specific probe Mitotracker Green (400 nM, 30 min). Three-dimensional images were obtained by confocal microscopy and then the Z-stacks of the thresholded images were volume-reconstituted as previously described (Parra et al., 2008; Parra et al., 2014). Our results showed that after 24 h, norepinephrine-treated cells presented a less connected mitochondrial network consistent with increased mitochondrial fission (Fig. 1A). These morphological observations were further confirmed by the quantification of the percentage of cells exhibiting a fragmented mitochondrial morphology, the mean relative volume of individual mitochondria and the relative number of mitochondria per cell. Fig. 1B (top panel) shows that norepinephrine significantly increased the percentage of cells that displayed fragmented mitochondria from 14 ± 1 (control, 0 h) to 39 ± 8 and 53 ± 8 after 24 and 48 h of norepinephrine incubation, respectively (mean \pm s.e.m.). Moreover, norepinephrine treatment also decreased the volume of individual mitochondria showing a 23 ± 8 decrease after 24 h (Fig. 1B, middle panel) and a further decrease after 48 h of norepinephrine incubation (46 ± 2). Conversely, the relative number of mitochondria per cell increased significantly by 48 ± 0.1 and 84 ± 1 at 24 and 48 h of norepinephrine treatment, respectively (Fig. 1B, lower panel).

To confirm these results, we performed indirect immunofluorescence to detect the endogenous mitochondrial protein mtHsp70 (also known as HSPA9) (Liu et al., 2003). By co-staining with phalloidin–Rhodamine, we were able to correlate mitochondrial network fragmentation with an increase in sarcomere structure and abundance in the cells treated with norepinephrine. As shown in Fig. 1C, the double staining revealed that cardiomyocytes exhibited a hypertrophic phenotype, determined as an increase in the cellular area and sarcomeric structure (Fig. 1D). Cardiomyocytes also presented an increase in the number of mitochondria per cell and a decrease in the mean mitochondrial area compared to controls (Fig. 1E).

Additionally, to establish whether the changes observed in the morphological structure of the mitochondrial network occurred in conjunction with a decrease in mitochondrial biogenesis or an increase in mitochondrial degradation, we evaluated mitochondrial mass by quantifying the total amount of the mitochondrial protein mtHsp70. As shown in supplementary material Fig. S1A, norepinephrine did not change the mtHsp70 levels measured by western blotting. This result was further confirmed using flow cytometry and the specific mitochondrial dye Mitotracker Green (supplementary material Fig. S1B). Taken together, these data strongly suggest that norepinephrine stimulates cardiomyocyte hypertrophy and also triggers fragmentation of the existing mitochondrial network without changing the existing balance between the rates of mitochondrial synthesis and turnover.

Norepinephrine decreases the mitochondrial function in cultured cardiomyocytes

Cardiomyocyte hypertrophy has been associated with decreased mitochondrial metabolism or functional capacity (Huss and Kelly, 2005; Neubauer, 2007). Therefore, we evaluated four different parameters of mitochondrial function in our norepinephrine-induced cardiomyocyte hypertrophy model. As shown in Fig. 2A–C, both mitochondrial membrane potential (Ψ_m) and the intracellular levels of ATP decreased after the treatment of

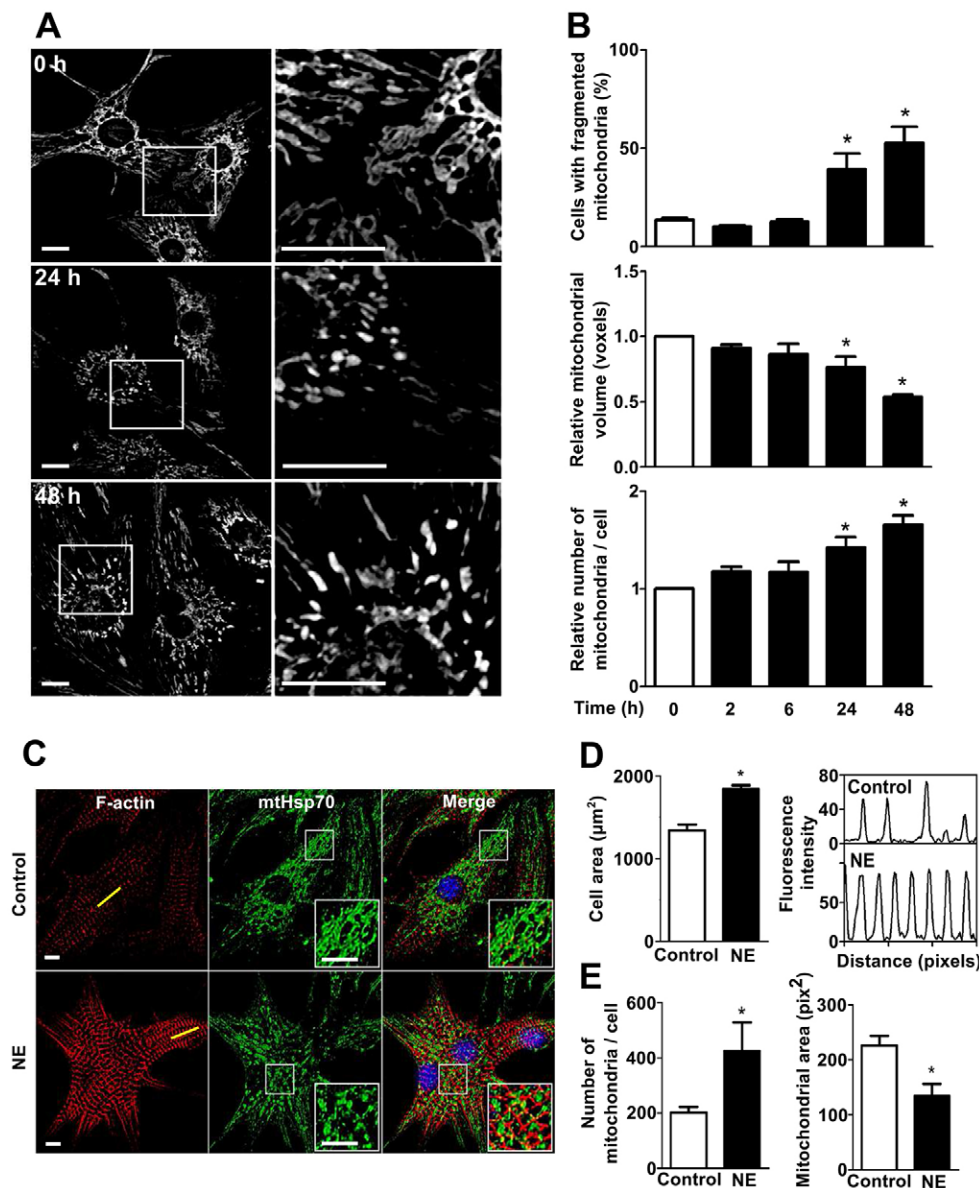


Fig. 1. The pro-hypertrophic factor norepinephrine stimulates mitochondrial fission in cultured cardiomyocytes. (A) Representative confocal images of the mitochondrial cardiomyocyte network in cells stained with Mitotracker Green and treated with norepinephrine (NE, 10 μM) for 0, 24 and 48 h (upper, middle and lower panel, respectively). The right column is a magnification of indicated areas in the left column. Scale bar: 10 μm . (B) Quantitative analysis (mean \pm s.e.m.; $n=5$) of mitochondrial morphology of cardiomyocytes treated with norepinephrine for the indicated times. Images were subjected to 3D reconstruction to determine the number and volume of mitochondrial particles. (C) Representative confocal images of cardiomyocytes treated with norepinephrine (0–48 h) and stained with phalloidine–Rhodamine to detect sarcomeric structures, and immunolabeled for the mtHsp70 protein to identify mitochondrial network. Scale bar: 5 μm . (D,E) Quantitative analysis (mean \pm s.e.m.; $n=3$) of (D) cell area and (E) mitochondrial morphology of cardiomyocytes treated as in C. The right-hand panel of D shows the intensity profile of the sarcomeric red fluorescence from the yellow line depicted in C. Number of mitochondria per cell, mitochondrial volume, mitochondrial area and cell area were evaluated with the ImageJ software. * $P<0.05$ versus control.

cardiomyocytes (48 h) with norepinephrine (-22% , $P<0.05$; and -25% , $P<0.05$, respectively). Whereas overall cellular reactive oxygen species (ROS) production was enhanced (39% , $P<0.05$), potentially reflecting mitochondrial dysfunction and increased loss of electrons through the electron transport chain. Importantly, the decreased mitochondrial function was not correlated with an increase in cell death in response to norepinephrine treatment as shown in supplementary material Fig. S1C.

To directly assess changes in mitochondrial oxidative phosphorylation (OXPHOS) we measured oxygen consumption rates in cardiomyocytes at baseline and under conditions of maximal uncoupling. Cardiomyocytes treated with norepinephrine showed a drop in both baseline and CCCP-uncoupled cellular oxygen consumption (Fig. 2D), decreasing the respiratory control ratio from 1.5 ± 0.14 to 1.2 ± 0.11 after 48 h (\pm s.e.m., $P<0.05$; supplementary material Fig. S1D). Taken together, these results indicate that norepinephrine both increases mitochondrial fragmentation and decreases mitochondrial function in cardiomyocytes.

Norepinephrine stimulates mitochondrial localization of Drp1 in cultured cardiomyocytes

To elucidate the mechanism of norepinephrine-dependent mitochondrial fission, changes in the levels of fusion and fission machinery proteins were assessed. Western blot analysis indicated that the abundance of either Drp1 or Fis1, two proteins central to the mitochondrial fission process, did not change after norepinephrine treatment, nor was there a significant change in the levels of either Mfn2 or OPA1, proteins of the mitochondrial fusion machinery (Fig. 3A,B). Because several studies have reported that loss of mitochondrial membrane potential enhances the cleavage of long isoforms of OPA1 (OPA1L), accumulating short protein isoforms (OPA1S) and promoting mitochondrial fission (Song et al., 2007; Ehses et al., 2009; Head et al., 2009), we also looked for changes in levels of specific OPA1 isoforms. However, no changes were found in the OPA1L:OPA1S ratio (Fig. 3B).

Previous studies (Yoon et al., 2003; Parra et al., 2008) have established the migration of Drp1 from the cytosol to Fis1-

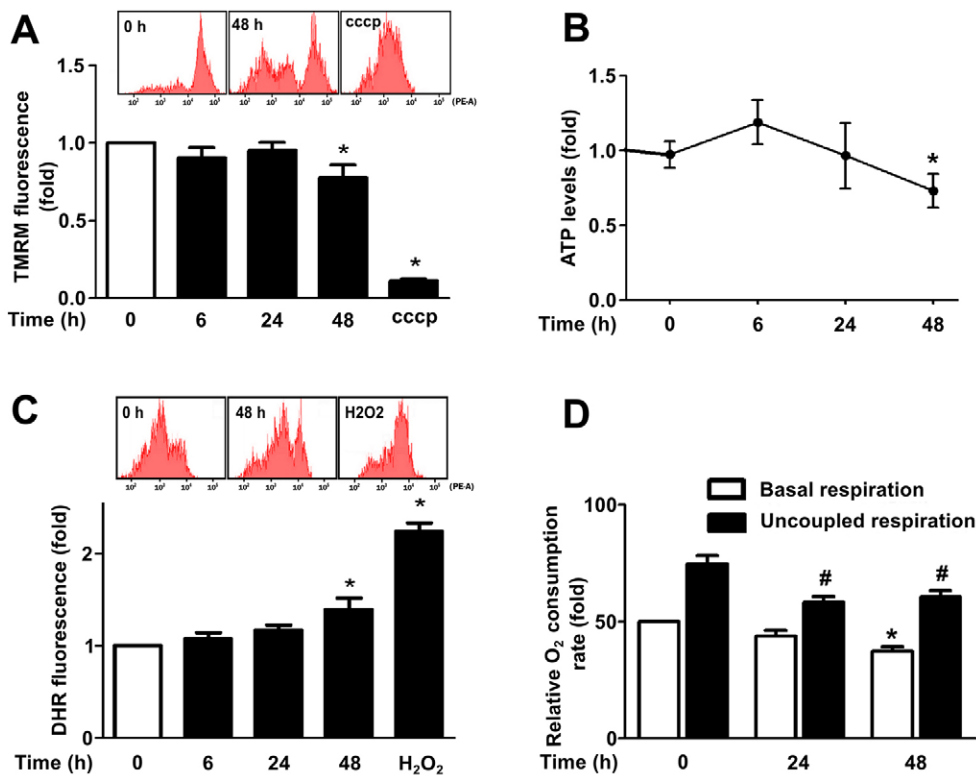


Fig. 2. Mitochondrial metabolism is decreased in hypertrophic cardiomyocytes. (A) Cells stimulated with norepinephrine (0–48 h) were incubated with tetramethylrhodamine (TMRM) to study mitochondrial membrane potential (Ψ_m) by flow cytometry. CCCP (10 μ M) was used as a positive control for mitochondrial depolarization (mean \pm s.e.m.; $n=4$). (B) Intracellular ATP content was determined using a luciferin-luciferase assay (mean \pm s.e.m.; $n=6$). (C) Total ROS content was measured by flow cytometry using the dihydrorhodamine (DHR) probe on cardiomyocytes treated with norepinephrine for the indicated times. H₂O₂ (100 μ M) was used as positive control (mean \pm s.e.m.; $n=4$). (D) Basal oxygen consumption (white bars) of cardiomyocytes stimulated with norepinephrine for 0–48 h was assessed with a Clark electrode. Uncoupled respiration rate (black bars) was determined by adding CCCP (200 nM) after 75% of the oxygen in the system had been depleted (mean \pm s.e.m.; $n=5$). * $P<0.05$ versus basal control; # $P<0.05$ versus uncoupled control.

containing fission points on the mitochondrial surface as an initial step in mitochondrial fragmentation. Therefore, we next evaluated whether mitochondrial fission triggered by norepinephrine was associated with changes in the distribution of Drp1. Our immunofluorescence studies indicated that the punctate distribution pattern of Drp1 was accentuated after 48 h of incubation with norepinephrine (Fig. 3C). At the same time, no changes in Fis1 content were observed, although the extent of colocalization of both proteins increased as evaluated by means of the Pearson's coefficient (R). Moreover, norepinephrine increased the effective colocalization of Drp1 with Fis1 ($P<0.05$), but not the effective colocalization of Fis1 with Drp1 (Fig. 3D), as evaluated by Manders' coefficients, thus suggesting that Drp1 migrates to mitochondria after norepinephrine stimulation, whereas Fis1 is associated with mitochondria under both conditions. To corroborate these results, mitochondrial protein fractions were isolated from cultured rat cardiomyocytes treated with norepinephrine for 0, 24 and 48 h. Then Drp1 protein levels were evaluated by western blotting. The results show an increase in Drp1 levels in the mitochondrial fractions of cardiomyocytes treated with norepinephrine for 48 h compared to controls (Fig. 3E).

Inhibition of mitochondrial fission prevents cardiomyocyte hypertrophy and decreased the mitochondrial dysfunction triggered by norepinephrine

In order to test whether the effects of norepinephrine on the mitochondrial fission machinery are relevant to its effects on mitochondrial function and cardiomyocyte growth, we next studied the impact of Drp1 inhibition on the cardiomyocyte response to norepinephrine. To this end, cells were transduced with adenoviruses encoding a dominant-negative mutant form of Drp1 (K38A) or a control adenovirus (LacZ) (supplementary material Fig. S2A). The Drp1K38A mutation affects GTPase activity and inhibits mitochondrial fission (Smirnova et al., 2001;

Liesa et al., 2008; Hernández-Alvarez et al., 2013). In agreement with earlier reports, Drp1K38A caused an increase in the baseline mitochondrial mean volume compared with LacZ-transduced cells (supplementary material Fig. S2). Importantly, the cells transduced with the control LacZ virus responded to norepinephrine with an increase in sarcomere abundance, sarcomere organization and cell size that was similar to non-transduced cells. In response to norepinephrine stimulation, Drp1K38A-transduced cardiomyocytes showed a decreased percentage of sarcomeric cells compared to LacZ-transduced cells ($43.5\% \pm 9.6$ vs $73.2\% \pm 11.4$, respectively, mean \pm s.e.m.) (Fig. 4A,B). There was no increase in cardiomyocyte cell area relative to vehicle-treated cells (Fig. 4C) and sarcomeric organization was reduced (Fig. 4D). Consistent with a reduction of hypertrophic growth, Drp1K38A blocked the norepinephrine-dependent increase in fetal cardiac β -myosin heavy chain (β -MHC) protein levels (Fig. 4E) and significantly decreased atrial natriuretic factor (ANF, encoded by *Nppa*) and RCAN 1.4 (exon 4 isoform encoded by the *Rcan1* gene) transcript levels (Fig. 4F), both classic markers of the hypertrophic response. Importantly, the drop in cardiomyocyte oxygen consumption rate in response to norepinephrine (48 h) was completely prevented in the cells transduced with Drp1K38A (Fig. 4G), suggesting that mitochondrial fission is a required step for norepinephrine-induced cardiomyocyte hypertrophy as well as the norepinephrine-induced reduction in mitochondrial functional capacity. To confirm this we used an alternative approach to promote mitochondrial fission (Fig. 5). Cardiomyocytes transduced with an antisense adenovirus targeting the fusion protein Mfn2 (AsMfn2) (Bach et al., 2003) displayed a fragmented mitochondrial network (supplementary material Fig. S3) along with an increase in the extent of sarcomerization and relative cell area (Fig. 5A–D). Moreover, transduction with the AsMfn2 adenovirus alone was sufficient to increase β -MHC protein levels, increase the ANF and RCAN 1.4 transcript levels, and decrease the consumption of oxygen (Fig. 5E–G), all changes similar to those seen

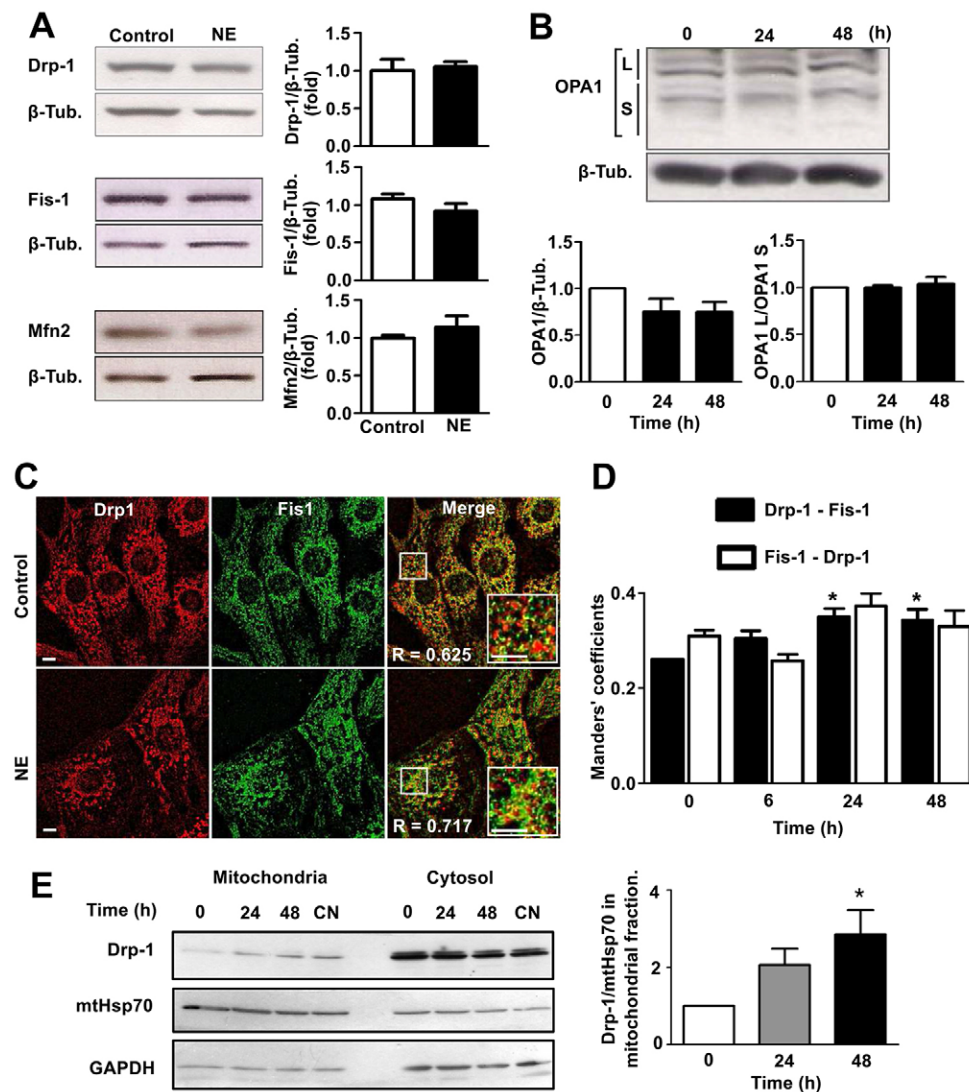


Fig. 3. Norepinephrine stimulates Drp1 translocation from cytosol to mitochondria.

(A) Protein levels of different mitochondrial dynamics machinery components were determined using western blotting in total extracts of cells stimulated with norepinephrine (NE, 0–48 h). Left panels show representative western blots. Right panels show quantification (mean ± s.e.m.; $n=6$). Values are relative to those of β -tubulin (β -Tub.). (B) Western blot showing the different OPA1 isoforms expressed in cardiomyocytes stimulated with norepinephrine for the indicated times (mean ± s.e.m.; $n=4$).

(C) Immunofluorescence images of cardiomyocytes treated as indicated, using anti-Drp1 (red) or anti-Fis1 (green) antibodies. R corresponds to Pearson's coefficient for fluorescence colocalization. Scale bar: 5 μ m. (D) Manders' coefficient quantification for immunofluorescence images of cells. Black and white bars indicate Drp1-associated fluorescence colocalization to Fis1 signal and Fis1-associated fluorescence colocalization to Drp1 signal, respectively. (mean ± s.e.m.; $n=4$). (E) Drp1 protein levels (mean ± s.e.m.; $n=4$) were determined by western blot assay in mitochondrial and cytosolic extracts from cardiomyocytes treated with norepinephrine for 0, 24 and 48 h or transfected with calcineurin adenovirus (CN). mtHsp70 and GAPDH were used as mitochondrial and cytosolic markers, respectively. * $P<0.05$.

in norepinephrine-treated cardiomyocytes. Collectively, these results suggest that mitochondrial fragmentation is sufficient to trigger changes in mitochondrial function and cardiomyocyte hypertrophy.

The α 1-adrenergic-receptor- Ca^{2+} -calcineurin pathway plays a key role in the mitochondrial fission stimulated by norepinephrine

Classically, norepinephrine-induced cardiomyocyte hypertrophy has been associated with the activation of α 1-adrenergic receptors and their second messenger Ca^{2+} (Frey et al., 2004). In this regard, the drug Prazosin (Praz), an α 1-adrenergic receptor antagonist used to treat high blood pressure and anxiety, has been shown to have beneficial effects in the treatment of hypertrophy induced by left ventricular pressure overload (Day et al., 1997; Perlini et al., 2006). Accordingly, pre-treatment of cardiomyocytes with Praz fully suppressed the mitochondrial fragmentation induced by norepinephrine, reducing the increase in the relative number of mitochondria per cell and preserving mitochondrial volume (Fig. 6A,B). Consequently, Praz also prevented the increase in intracellular Ca^{2+} levels observed after norepinephrine treatment (Fig. 6C). Ca^{2+} has been identified as an important second messenger in the development of cardiomyocyte hypertrophy downstream of α 1-adrenergic

receptors. In this pathway, activation of phospholipase C promotes release of internal Ca^{2+} stores, which in turn activates calcineurin, known to play a central role in hypertrophy and pathological cardiac remodeling. Calcineurin and its transcription factor target, nuclear factor of activated T cells (NFAT), increase the expression of the exon 4 isoform of the *Rcan1* gene, which encodes an endogenous feedback inhibitor of calcineurin activity (Rothermel et al., 2003). RCAN1.4 protein levels were elevated in cardiomyocytes treated with norepinephrine (Fig. 6D) consistent with a model in which norepinephrine stimulation promotes downstream activation of calcineurin.

Distinct post-translational modifications of Drp-1 regulate its activation and translocation to mitochondria (Santel and Frank, 2008). Phosphorylation by cyclic-AMP-dependent protein kinase (PKA) at Ser637 in the GTPase effector domain of Drp-1 decreases its GTPase activity reducing mitochondrial fission (Santel and Frank, 2008). Phosphorylation of this PKA-dependent site can be reversed by calcineurin, thus promoting its translocation to mitochondria and engaging mitochondrial fission (Chang and Blackstone, 2007; Cribbs and Strack, 2007). The treatment of cardiomyocytes with norepinephrine for 48 h decreased the phosphorylation of Drp-1 at Ser637 (Fig. 6E), thus connecting the development of hypertrophy and the activity of

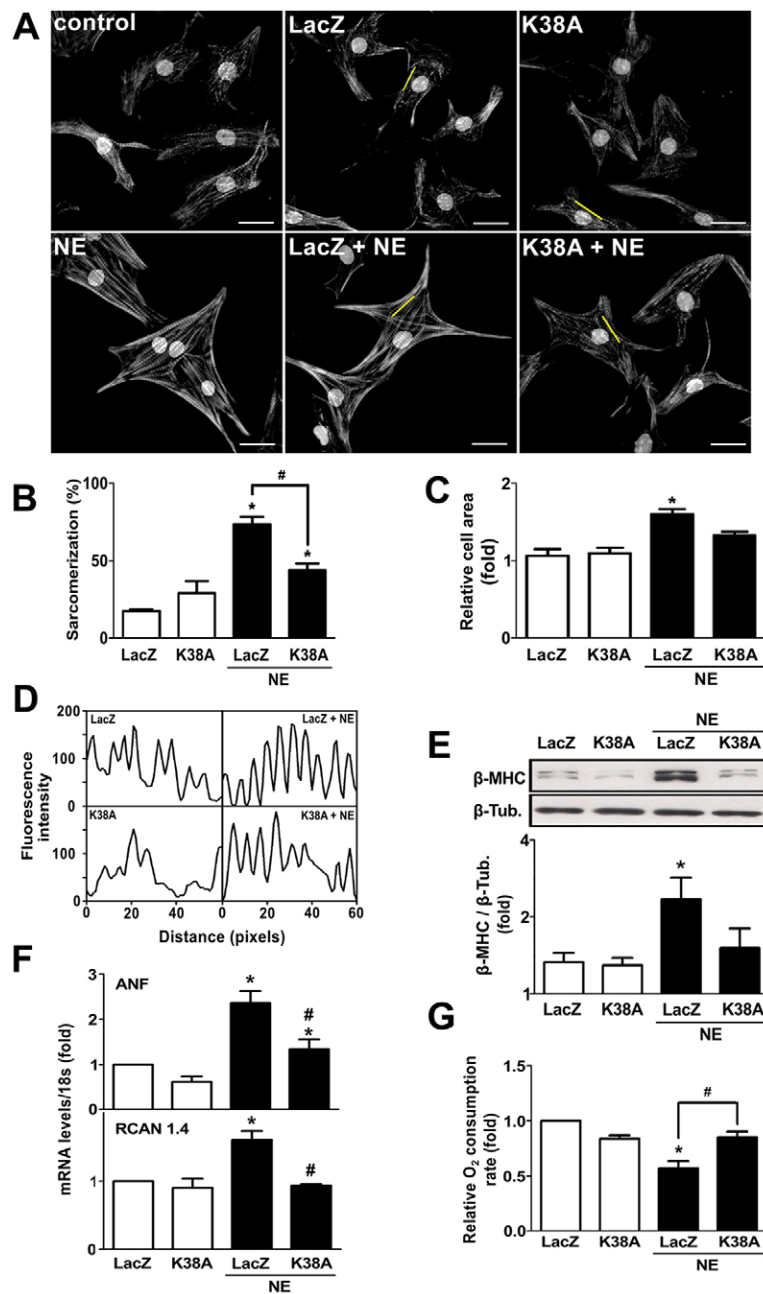


Fig. 4. Dominant-negative Drp1 (K38A) prevents norepinephrine-induced cardiomyocyte hypertrophy.

(A) Representative fluorescence microscopy images of cardiomyocytes transfected with a LacZ- or K38A-encoding adenovirus prior to norepinephrine (NE) stimulation for 48 h, and stained with phalloidin–Rhodamine for sarcomeric detection. Nuclei were stained with Hoescht 33342. Scale bar: 20 μ m. (B) Percentage of sarcomerized cardiomyocytes and (C) cell area were calculated using at least 55 cells per condition (mean \pm s.e.m.; $n=4$). (D) Fluorescence intensity profile of the yellow lines depicted on A. (E) Western blot analysis of the hypertrophic biomarker β -MHC on cells treated with norepinephrine for 48 h after LacZ or K38A adenovirus transduction (mean \pm s.e.m.; $n=3$). (F) Determination of mRNA levels of atrial natriuretic factor (ANF) and RCAN 1.4 using qPCR (mean \pm s.e.m.; $n=3$). (G) Basal oxygen consumption of Drp1-K38A-transduced cardiomyocytes and stimulated with norepinephrine for 48 h (mean \pm s.e.m.; $n=4$). * $P<0.05$ versus non stimulated control; # $P<0.05$ versus norepinephrine-stimulated control.

calcineurin with the activation of mitochondrial fission at the level of Drp1.

Next, to further define the connection between mitochondrial fission and hypertrophic remodeling induced by norepinephrine, we used two approaches to test the dependence of mitochondrial network fragmentation on calcineurin activity: (1) an adenovirus encoding a noncompetitive calcineurin inhibitory peptide (CAIN), and (2) an adenovirus encoding a constitutively active calcineurin (Delling et al., 2000; Yoon et al., 2003; Jofuku et al., 2005). Both CAIN and the constitutively active calcineurin adenoviruses were tested for their ability to decrease or increase RCAN1.4 protein levels, respectively (supplementary material Fig. S4A,B). The transduction of cardiomyocytes with the adenovirus CAIN decreased all the effects of norepinephrine on mitochondrial morphology (Fig. 7A,B), preventing the increase

in the percentage of cells displaying fragmented mitochondria, as well as the decrease in mitochondrial relative volume and the increase in the number of mitochondria per cell. Conversely, transduction of cells with the constitutively active calcineurin adenovirus, increased mitochondrial network fragmentation as assayed by the same parameters described previously (Fig. 7A,B) and, conversely, there was an increase in the amount of Drp1 protein fractionating with mitochondria (Fig. 3E). Furthermore, the CAIN adenovirus also prevented the drop in the oxygen consumption rate induced by norepinephrine (Fig. 7C). Taken together, these results are the first to connect the development of calcineurin-dependent hypertrophy with mitochondrial network fragmentation and the mitochondrial metabolic alterations observed during the onset of this pathological state.

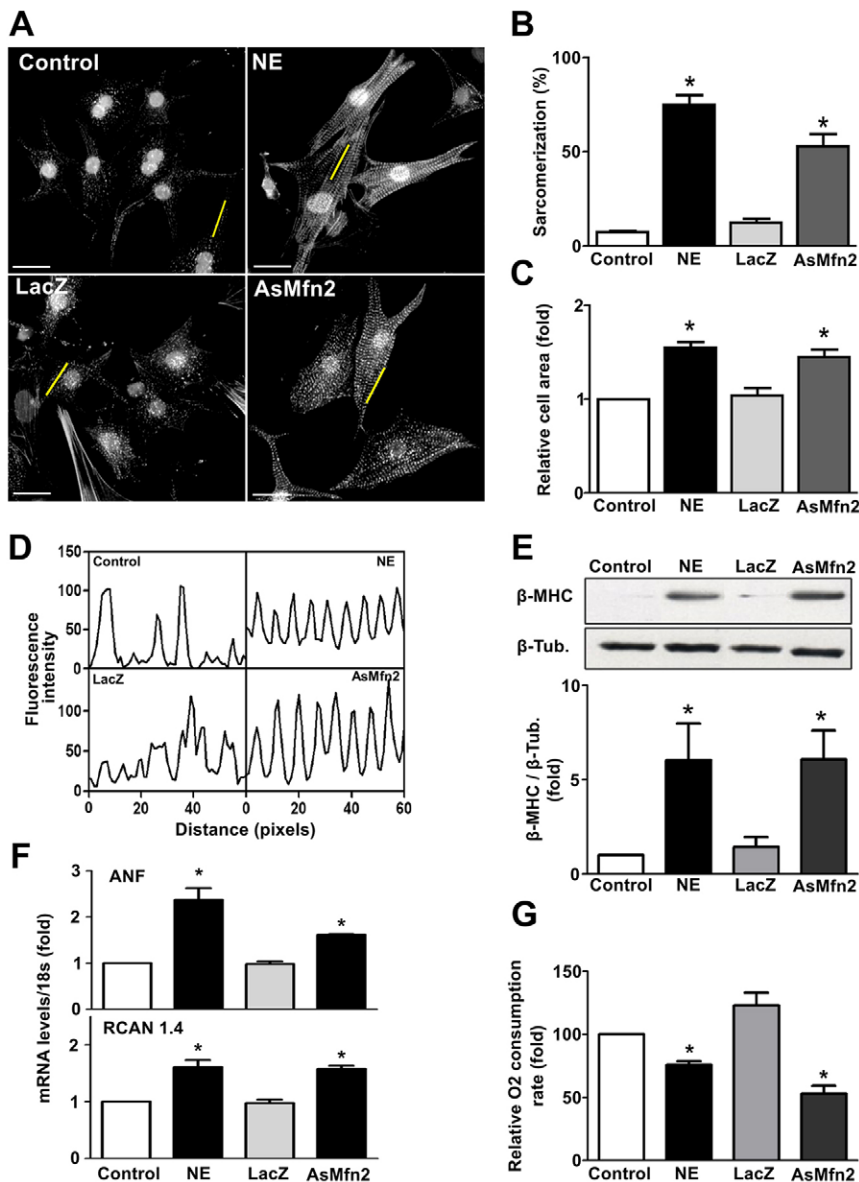


Fig. 5. Lack of Mfn2 induces cardiomyocyte hypertrophy. (A) Cells were transduced with LacZ or Mfn2 antisense (AsMfn2) adenovirus or norepinephrine (NE) for 48 h and then stained with phalloidin–Rhodamine and Hoechst 33342 to visualize sarcomeric organization and nuclei, respectively. Scale bar: 20 μ m. (B) Percentage of highly sarcomerized cardiomyocytes and (C) cell area was determined using at least 55 cells per condition (mean \pm s.e.m.; $n=4$). (D) Fluorescence intensity profile of the yellow lines depicted on A. (E) Western blot for β -MHC on cells treated with norepinephrine or transduced with the indicated adenovirus. A quantification is shown in the lower panel (mean \pm s.e.m.; $n=4$). (F) mRNAs levels for ANF and RCAN 1.4 of AsMfn2-transduced cardiomyocytes (mean \pm s.e.m.; $n=4$). * $P<0.05$ versus their respective control; # $P<0.05$ versus norepinephrine-LacZ. (G) Basal oxygen consumption of AsMfn2-transduced cardiomyocytes (mean \pm s.e.m.; $n=4$). * $P<0.05$ versus their respective controls.

A recent paper using cardiomyocyte-specific Mfn2-knockout mice showed that Mfn2 plays a role in mitophagy (Chen and Dorn, 2013). This process requires a mitochondrial fusion and fission balance to produce mitochondria small enough to be subject to degradation (Twig et al., 2008). Mitophagy is the basis of mitochondrial quality control and therefore crucial for maintaining a fully functional network. To address the possible participation of mitophagy in our model, we tested whether our experimental strategy also stimulates mitophagy. Either norepinephrine treatment or infection with the AsMfn2 antisense adenovirus increased the colocalization of Parkin with mitochondria (supplementary material Fig. S4C,D), consistent with activation of mitophagy. This agrees with our previous work demonstrating that depletion of Mfn2 from skeletal muscle cells increased colocalization of LysoTracker Red with a mitochondrial marker, suggesting that the disruption of the continuity of the mitochondrial network increases mitochondrial turnover (del Campo et al., 2014).

Finally, to investigate whether a metabolic change directly enhances hypertrophy, we tested the effect of a respiratory

mitochondrial inhibitor in the development of cardiomyocyte hypertrophy. To this end, cultured rat cardiomyocytes were treated with the ATP synthase inhibitor oligomycin (0.2–2 μ M) for 48 h. Cells were then fixed and stained with phalloidin–Rhodamine to determine cell area as a hypertrophic parameter. As shown in supplementary material Fig. S4F, the results do not show significant changes in the induction of hypertrophic response. However, future studies should investigate in more detail whether a direct mitochondrial metabolic stress stimulates the onset of cardiomyocyte hypertrophy.

DISCUSSION

There is a strong association between cardiac pathologies and changes in mitochondrial form and function. As a high-energy demanding tissue, cardiac muscle might be particularly sensitive to any dysregulation of metabolism (Kuzmicic et al., 2011). Mitochondrial dynamics are key determinants of mitochondrial form and function but their role in the progression of cardiac diseases is not yet fully understood. Furthermore, little is known with respect to how mitochondrial morphology changes during

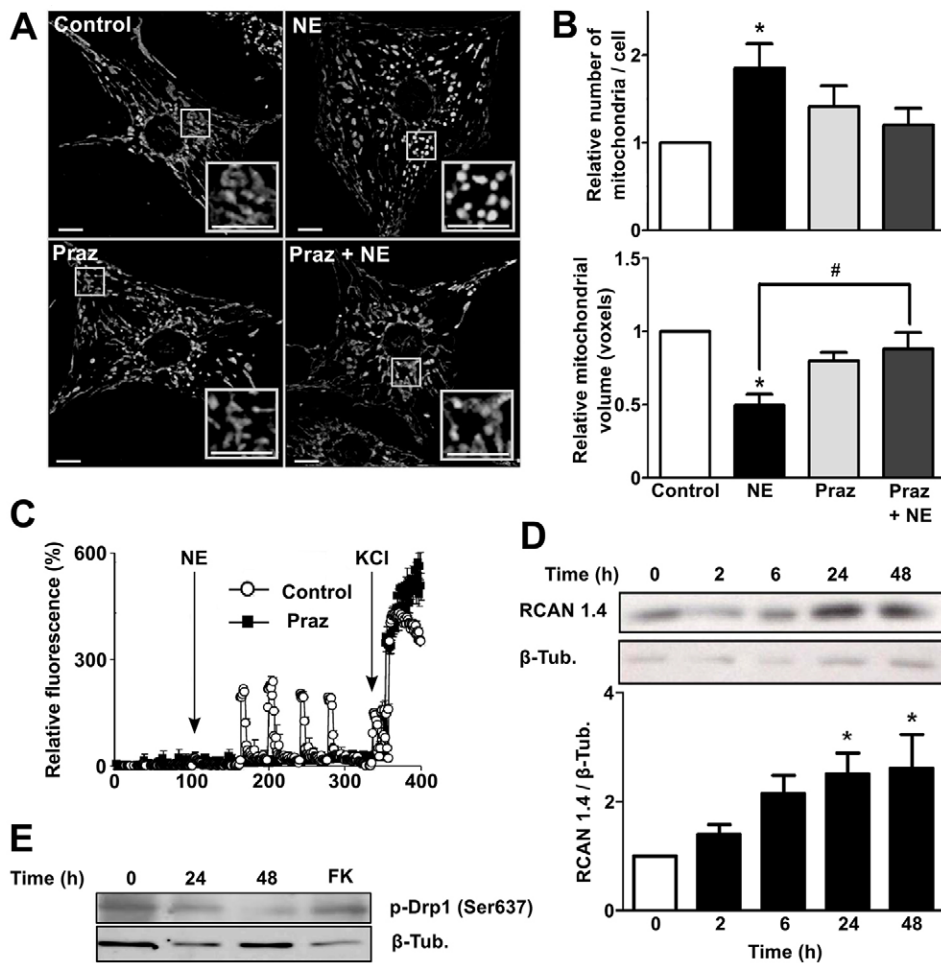


Fig. 6. Norepinephrine activates α_1 -adrenergic receptor signaling to promote mitochondrial fission on cultured cardiomyocytes. (A) Representative confocal microscopy images of cells stimulated with norepinephrine (NE) for 48 h and/or treated with the α_1 -adrenergic receptor antagonist Prazosin (Praz, 1 μ M), and then stained with Mitotracker Green to visualize mitochondrial network. Scale bar: 5 μ m. (B) Quantitative analysis of the mitochondrial morphology of cells treated with norepinephrine for 48 h and/or Praz (mean \pm s.e.m.; $n=7$). (C) Fluorescence profile of cardiomyocytes incubated with fluo3AM (5.4 μ M) to visualize cytosolic Ca²⁺ increases in response to norepinephrine. White circles and black squares show control cells and cardiomyocytes preincubated with Praz for 30 min, respectively. The arrows show the time of norepinephrine stimulation followed by the addition of KCl as a positive control to increase cytosolic Ca²⁺ levels by sarcoplasmic depolarization. (D) Western blots for RCAN 1.4, as a calcineurin activity reporter, in cells stimulated with norepinephrine (0–48 h). A quantification is presented in the lower panel (mean \pm s.e.m.; $n=4$). (E) Representative western blot ($n=3$) for phospho-Drp1 (Ser637) protein. Forskolin (FK) was used as a positive phosphorylation control. * $P<0.05$ versus control or $t=0$; # $P<0.05$ versus norepinephrine-stimulated cells.

hypertrophic growth of cardiomyocytes or the mechanisms that control the process. It is clear, however, that such changes occur because a fragmented mitochondrial phenotype has been observed in diverse pathological models of cardiac remodeling or heart failure (Chen et al., 2009; Ong et al., 2010).

The data presented here suggest a role for mitochondrial fission in the development of catecholamine-induced cardiac hypertrophy and demonstrate the potential of preserving mitochondrial fusion as an approach to cardioprotection. By using multiple independent assessments, we demonstrated that treatment with norepinephrine caused changes in mitochondria indicative of reduced functional capacity. These included a decrease in oxygen consumption, a decrease in mitochondrial membrane potential and a reduction in total cellular ATP levels. Importantly, fragmentation of the mitochondrial network preceded these metabolic alterations in response to norepinephrine. We did not observe any changes in the levels of mitochondrial fission and fusion proteins in neonatal rat cardiomyocytes treated with norepinephrine. This suggests that the changes seen in mitochondrial morphology and function were due to changes in the regulation of the activity of the fission and fusion machinery rather than due to changes in the abundance of individual components. This is contrary to a number of previous studies reporting changes in the protein or mRNA levels of several proteins involved in mitochondrial dynamics under various hypertrophic conditions (Fang et al., 2007; Chen et al., 2009; Javadov et al., 2011). The reason for these contrasting findings might lie in the specifics of the

experimental system or severity of stimulus. We specifically chose to use norepinephrine at a concentration sufficient to induce hypertrophic growth but that did not compromise cell viability. This allowed us to examine mitochondrial and metabolic remodeling independently of the activation of cell death pathways.

The fission process requires the recruitment of cytosolic Drp1 to mitochondria and the subsequent fragmentation of the mitochondrial network by membrane constriction (Smirnova et al., 2001). The importance of Drp1 in the development of cardiac diseases has been demonstrated in other studies. Ashrafian et al. have observed that transgenic mice with a mutation in the middle portion of Drp1 (mutation that alters the interaction between Drp1 monomers), developed ventricular wall thinning, interstitial fibrosis and a significant decrease in contractile function (Ashrafian et al., 2010), demonstrating that Drp1-mediated processes are essential for the maintenance of normal cardiac function. Another study showed that during periods of cardiac ischemia in mice, mitochondrial fission occurs in a Drp1-dependent manner. Furthermore, the use of a pharmacological inhibitor for Drp1, mdivi-1, prevented fragmentation of the mitochondrial network, reduced cell death and was associated with both a decrease in the opening of the mitochondrial permeability transition pore and the preservation of mitochondrial membrane potential during post-ischemia reperfusion (Ong et al., 2010). Related studies showed that mdivi-1 treatment ameliorated pressure overload-induced heart failure in mice subjected to ascending-aorta banding (Givvimani

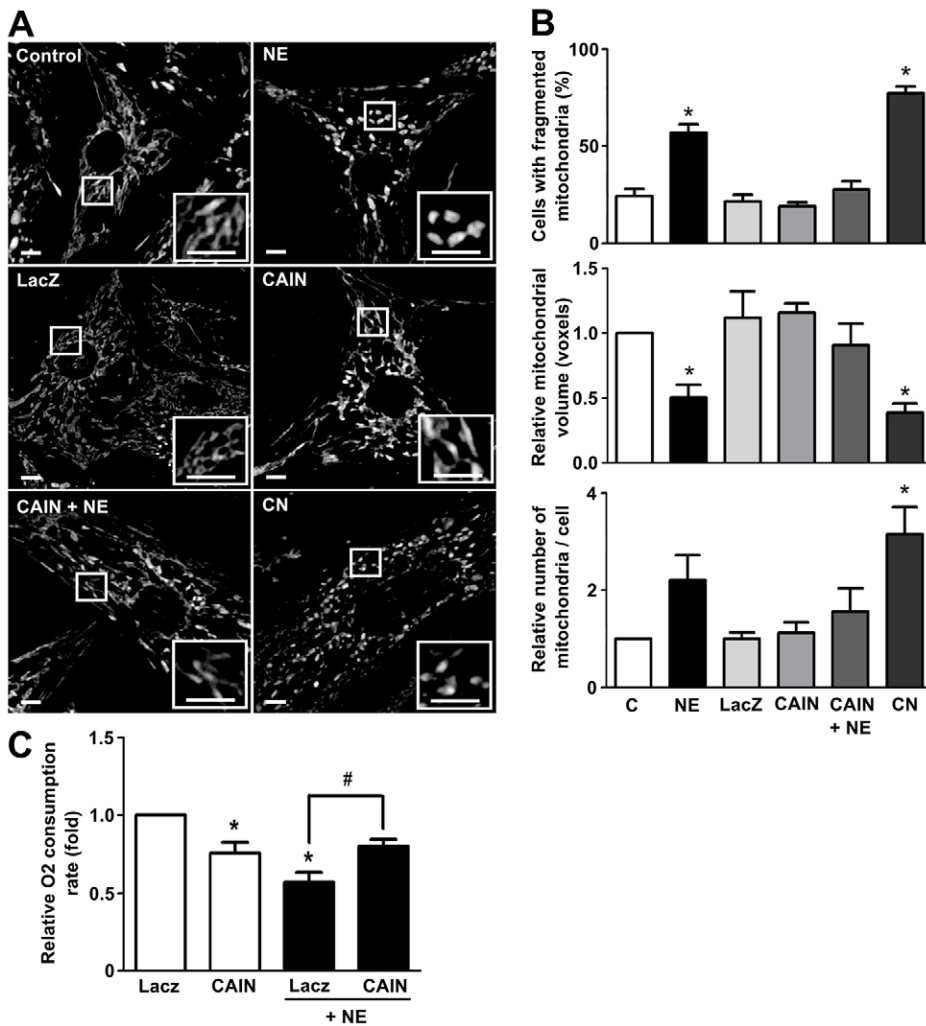


Fig. 7. Calcineurin activation induces mitochondrial fission in cultured cardiomyocytes. (A) Representative confocal microscopy images of cells stained with Mitotracker Green after transduction with the adenovirus containing LacZ, CAIN or calcineurin (CN) and after norepinephrine (NE) stimulus (48 h). Scale bar: 5 μ m. (B) Quantitative analysis of confocal microscopy images of cell treated as in A to evaluate mitochondrial morphology (mean \pm s.e.m.; n=4). (C) Oxygen consumption assays of cardiomyocytes transduced with the indicated adenovirus and stimulated with norepinephrine for 48 h (mean \pm s.e.m.; n=4). * P <0.05 versus non stimulated control; # P <0.05 versus norepinephrine-stimulated control.

et al., 2012). Taken together, these results suggest that a reduction in Drp1-mediated mitochondrial fission can prevent detrimental changes in development of cardiac pathologies but insinuate that a complete loss of Drp1 function can likewise be detrimental. Our results reinforce this concept by showing that the inhibition of mitochondrial fission, with a dominant negative adenovirus for Drp1, prevents hypertrophy in neonatal cardiomyocytes, acting not only to blunt hypertrophic growth, but also to prevent norepinephrine-mediated reductions in mitochondrial function. These findings support a model in which Drp1 plays a crucial role in the development of heart diseases.

The fact that an antisense adenovirus against the fusion protein Mfn2, as an alternative approach to increase mitochondrial fission, was sufficient to stimulate hypertrophic growth of cardiomyocytes, in the absence of external stimuli, suggests that it is a change in the overall balance between fission and fusion itself that might mediate the hypertrophic response, rather than some specific function of Drp1 apart from its role in control of mitochondrial dynamics. Consistent with our findings, Mfn2-deficient mice display cardiac hypertrophy accompanied by eventual functional deterioration (Papanicolaou et al., 2011). In addition to its role in mitochondrial fusion, Mfn2 also participates in various cellular processes. For example, de Brito and Scorrano found that Mfn2 directly interacts with Ras and inhibits the Ras–Raf–MEK–ERK1/2 pathway (de Brito and Scorrano, 2009).

Furthermore, decreased levels of Mfn2 in MEFs increased the phosphorylation of ERK1/2 (de Brito and Scorrano, 2009), and activation of ERK1/2 is known to be sufficient to promote a hypertrophic growth in cardiomyocytes (Ramirez et al., 1997; Bueno et al., 2000; Clerk et al., 2006). Mfn2 also participates in the interaction between mitochondria and ER, which is essential for maintaining proper mitochondrial Ca^{2+} uptake and the subsequent stimulation of mitochondrial metabolism (de Brito and Scorrano, 2009; Cárdenas et al., 2010; Bravo et al., 2013).

Sustained calcineurin activation has been shown to be sufficient to promote cardiac hypertrophy both *in vitro* and *in vivo* (Molkentin et al., 1998). Calcineurin activity can also lead to an increase in mitochondrial fission through mechanisms involving dephosphorylation of Drp1 at Ser637 (Cereghetti et al., 2008). This study demonstrates that stimulation of the α_1 -adrenergic receptor by norepinephrine leads to an increase in cytoplasmic Ca^{2+} levels and activation of calcineurin, culminating in subsequent fragmentation of the mitochondrial network. Remarkably, the dominant-negative Drp1 mutant not only blocked mitochondrial fission in response to norepinephrine, it also inhibited hypertrophic growth. By contrast, inhibition of calcineurin prevented mitochondrial fission in response to norepinephrine, suggesting that both mitochondrial fission and hypertrophic growth might be directly linked through cross talk of Ca^{2+} /calcineurin-dependent processes. For instance, increased

mitochondrial fission has been associated with a decrease in the Ca^{2+} uptake capacity of the mitochondria (de Brito and Scorrano, 2008). Such a reduction in mitochondrial Ca^{2+} buffering capacity could potentially lead to a subsequent increase in cytosolic Ca^{2+} or an increase in the duration of a cytoplasmic Ca^{2+} signal. Could such a mechanism feed-forward to prolong or sustain calcineurin activation sufficiently to bring about hypertrophic growth? The data presented here are consistent with this and provide the groundwork for further investigation to test such a model.

The interdependence of calcineurin-mediated hypertrophy and mitochondrial network fragmentation during the onset of hypertrophy might give insight into the mechanism of action of recent studies examining the role of micro RNA-499 (miR-499) in cardiac hypertrophy. miR-499 has been shown to target the catalytic subunit of calcineurin, therefore inhibiting Drp1 dephosphorylation and thus both inhibiting hypertrophic growth and decreasing mitochondrial fragmentation (Wang et al., 2011). Interestingly, increased expression of miR-499 protects the heart from changes during ischemia reperfusion, similarly to pharmacological inhibition of fission using mdivi-1. Taken together with our results, these studies argue in favor of promoting mitochondrial fusion as a protective strategy in calcineurin-dependent heart disease.

In our study we identify the following limitations: (1) AsMfn2 acts by blocking mitochondrial fusion rather than by actively promoting mitochondrial fission, therefore, future studies should be designed to promote mitochondrial fission directly by overexpression of Mff (Gandre-Babbe and van der Blik, 2008; Otera et al., 2010) to determine whether promoting mitochondrial fission has the same consequence as blocking fusion; and (2) Mfn2 has a variety of functions in addition to its role in mitochondrial fusion. Repression of Mfn1 function as described by Papanicolaou et al. (Papanicolaou et al., 2012) could be used to further pursue the specific role of mitochondrial fusion in regulation of cardiomyocyte hypertrophy.

In conclusion, the present study demonstrates a close relationship between mitochondrial dynamics and the development of cardiac hypertrophy, showing that norepinephrine promotes mitochondrial fission by the activation of the α_1 -adrenergic-receptor- Ca^{2+} -calcineurin-Drp1 signaling pathway resulting in a decrease in mitochondrial metabolism and function. Importantly, we demonstrate that controlling the balance between mitochondrial fission and fusion is sufficient to promote or prevent cardiomyocyte hypertrophy. These new findings suggest a mechanism through which mitochondrial dynamics could play a key role in hypertrophic growth and pathological remodeling of the heart. Furthermore, our work identifies intervention of mitochondrial dynamics as a new potential therapeutic target for the prevention or control pathological cardiac hypertrophy.

MATERIALS AND METHODS

Reagents

Antibodies against OPA1 and Mfn2 were purchased from Abcam; anti-Drp1 antibody was obtained from BD Transduction Laboratories. Parkin antibody was obtained from Millipore (05-882). Fis1 antibody was purchased from Alexis Biochemicals. Antibody against phosphorylated Drp1 (Ser637) was purchased from Cell Signaling (4867s) and mtHsp70 was from Affinity BioReagents. Tetramethylrhodamine methyl ester (TMRM), Mitotracker Green FM, FBS and Alexa Fluor secondary antibodies were from Invitrogen. The antibodies against RCAN 1.4, β -tubulin and α -actin, as well as the reagents norepinephrine, oligomycin, dihydrorhodamine 123, carbonyl cyanide m-chlorophenylhydrazone (CCCP), Dulbecco's modified Eagle's medium (DMEM), M199

medium and others were purchased from Sigma-Aldrich. Protein assay reagents were from Bio-Rad. The generation and use of AsMfn2 and Drp1K38A was previously described (Bach et al., 2003; Liesa et al., 2008; Hernández-Alvarez et al., 2013). Adenovirus CAIN and calcineurin were kindly provided by Jeffrey D. Molkentin (Division of Molecular Cardiovascular Biology, Children's Hospital Medical Center, Cincinnati, USA). Cardiomyocytes were transduced with adenoviral vectors at a multiplicity of transduction (MOI) of 300, 24 h before norepinephrine treatment. Adenovirus LacZ was used as control.

Cardiomyocyte hypertrophy evaluation

Sarcomerization was determined by epifluorescence microscopy analysis (Carl Zeiss Axiovert 135, LSM Microsystems) of methanol-permeabilized cells stained with phalloidin-Rhodamine (1:400; F-actin staining) as previously described (Munoz et al., 2010). At least 50 cells from randomly selected fields were analyzed using the ImageJ software (NIH).

ATP measurement

Cells were plated in gelatine-coated 96-well plates and ATP content was determined using a luciferin/luciferase based assay (Cell-Titer Glo Kit, Promega) (Chiong et al., 2010).

Cell viability assay

The integrity of the plasma membrane of cardiomyocytes was assessed by the ability of cells to exclude propidium iodide). Cells were washed once with PBS and dyed with 0.1 mg/ml propidium iodide. The levels of propidium iodide incorporation were quantified on a FACScan flow cytometer. Cell size was evaluated by forward-angle light scattering (FSC). PI-negative cells of normal size were considered alive (Criollo et al., 2007; Maramba et al., 2010).

Culture of neonatal rat cardiomyocytes

Cardiomyocytes were isolated from hearts of neonatal Sprague-Dawley rats as described previously (Galvez et al., 2001). Rats were bred in the Animal Breeding Facility of the University of Chile. All the experiments were in agreement to the *Guide for the Care and Use of Laboratory Animals* published by the US National Institutes of Health (2011) and approved by our Institutional Ethics Review Committee. Cardiomyocytes were plated at a final density of 1×10^3 – $8 \times 10^3/\text{mm}^2$ on gelatin-coated 35, 60 or 100 mm Petri dishes. For fluorescence measurements, cells were plated on gelatin-coated 25 mm glass coverslips in 35-mm Petri dishes. Once primary cell cultures of cardiomyocytes were obtained they were incubated with or without norepinephrine (10 μM) for 0–48 h in DMEM and M199 (4:1) medium, in the presence or absence of the different inhibitors or reagents. Cultured cardiomyocytes were identified using an anti- β -MHC antibody and cell cultures were at least 95% pure.

Analysis of Ψ_m and ROS by flow cytometry

Ψ_m and ROS were measured after loading cardiomyocytes with tetramethylrhodamine methyl ester (200 nM, 30 min), as previously described (Munoz et al., 2010), or dihydrorhodamine 123 (100 μM , 30 min), respectively. Cell fluorescence was determined by flow cytometry using a FACScan system (Becton-Dickinson).

Immunofluorescence studies and colocalization analysis of Drp1, Fis1 and Parkin

Cells cultured on gelatin-coated coverslips were fixed with PBS containing 4% paraformaldehyde and incubated for 10 min in ice-cold 0.1% Triton X-100 for permeabilization. Nonspecific sites were blocked with 1% BSA in PBS for 1 h and then the cells were incubated with antibodies against Drp1 (1:500), Fis1 (1:1000), Parkin (1:500) or mtHsp-70 (1:500). Secondary antibodies were Alexa-Fluor-488-conjugated anti-mouse-IgG for Drp1 and Parkin or mtHsp-70 and Alexa-Fluor-456-conjugated anti-rabbit-IgG for Fis1 (1:600). For the colocalization analysis only one focal plane was analyzed with a Zeiss LSM-5, Pascal 5 Axiovert 200 microscope. Images obtained were deconvolved and background was subtracted using the ImageJ software. Colocalization

between the proteins was quantified using the Manders' algorithm, as previously described (Manders et al., 1993; Costes et al., 2004; Parra et al., 2008; Ramirez et al., 2010).

Mitochondrial isolation

Cardiomyocytes (7×10^6) were cultured in 10-cm Petri dishes. After treatment, mitochondria were fractionated using a mitochondrial isolation kit for cultured cells (Abcam) according to the manufacturer's instructions. To ensure the purity of the fraction, the presence of mtHsp70 and GAPDH were used as a mitochondrial and cytosolic markers, respectively.

Measurement of cytoplasmic Ca^{2+}

To determine cytoplasmic Ca^{2+} levels, images were obtained from cultured cardiomyocytes preloaded with fluo3 am using an inverted confocal microscope (Carl Zeiss LSM-5, Pascal 5 Axiovert 200 microscope). Cardiomyocytes were washed three times with Ca^{2+} -containing resting medium (Krebs buffer) to remove DMEM/M199 culture medium, and loaded with 5.4 μ M fluo3 am for 30 min at room temperature. After loading, cells were washed either with the same buffer and used within 2 h. Cells containing coverslips were mounted in a 1 ml capacity chamber and placed in the microscope for fluorescence measurements after excitation with a laser line of 488 nm. Norepinephrine was quickly (less than 1 s) added to the chamber. The fluorescent images were collected every 1 s and analyzed frame by frame with Image J software (NIH, Bethesda, MD). To quantify fluorescence, the summed pixel intensity was calculated from the section delimited by the contour of a whole cell. Intracellular Ca^{2+} levels were expressed as relative total fluorescence [$\Delta F/F_0$, ratio of fluorescence difference, stimulated-basal ($F_i - F_0$), to basal value (F_0)] as a function of time. The fluorescence intensity increases proportionally with intracellular Ca^{2+} (Ibarra et al., 2004; Chiong et al., 2010). Digital image processing was performed as previously described (Ibarra et al., 2004; Chiong et al., 2010). Under our experimental conditions (0–100 s), no photobleaching was observed.

Mitochondrial dynamics analysis

Cells were incubated for 30 min with Mitotracker Green FM (400 nM) and maintained in Krebs solution. Confocal image stacks were captured with a Zeiss LSM-5, Pascal 5 Axiovert 200 microscope, using LSM 5.3.2 image capture and analysis software and a Plan-Apochromat 63 \times 1.4 NA oil DIC objective, as previously described (Parra et al., 2008; Parra et al., 2014). Images were deconvolved with Image J (NIH) and then, z-stacks of thresholded images were volume-reconstituted using the VolumeJ plug-in. The number and individual volume of each object (mitochondria) were quantified using the ImageJ-3D Object counter plug-in. Once individual mitochondrial volume was obtained for each mitochondrial particle, the values were averaged and are expressed relative to the controls. A decrease in mean mitochondrial volume together with an increase in the number of mitochondria was considered as fission criteria (Szabadkai et al., 2004; Yu et al., 2006). The percentage of cells with a fragmented pattern was also determined (Yu et al., 2006). Each experiment was performed at least four times and 16–25 cells per condition were quantified.

Oxygen consumption determination in live cells

Cells plated on 60-mm gelatine-coated dishes were trypsinized and then re-suspended in PBS. The cells were placed in a sealed chamber at 25 $^{\circ}$ C, coupled to a Clark electrode 5331 (Yellow Springs Instruments). Data obtained correspond to the amount of oxygen remaining in the chamber in time. Cells were maintained in the chamber for 20 min in order to calculate the rate of oxygen consumption.

Analysis of mRNAs by qPCR

Real-time PCR was performed with SYBR green (Applied Biosystems) as previously described (Parra et al., 2014). Data for each transcript were normalized to 18S rRNA as internal controls with the 2- $\Delta\Delta$ Ct method. Primers used were as follows: ANF rat forward,

5'-CTTCTTCCTTCCTGGCCT-3', and reverse, 5'-TTCATCGGTC-TGCTCGCTCA-3'; and RCAN1.4 rat forward, 5'-CCCCTGAAAAG-CAGAATGC-3'; RCAN1.4, and rat reverse 5'-TCCTTG TCATAT-GTTCTGAAGAGGG-3'.

Western blot analysis

Equal amounts of protein from cells were separated by SDS-PAGE (10% polyacrylamide gels) and electrotransferred to nitrocellulose. Membranes were blocked with 5% milk in Tris-buffered saline, pH 7.6, containing 0.1% (v/v) Tween 20 (TBST). Membranes were incubated with primary antibodies at 4 $^{\circ}$ C and re-blotted with horseradish peroxidase-linked secondary antibody [1:5000 in 1% (w/v) milk in TBST]. The bands were detected using ECL with exposure to Kodak film and quantified by scanning densitometry. Protein content was normalized by β -tubulin or mtHsp70 levels.

Statistical analysis

Data are shown as mean \pm s.e.m. for the number of independent experiments indicated (*n*) and represent experiments performed on at least three separate occasions. Data were analyzed by one-way ANOVA and comparisons between groups were performed using a protected Tukey's test. Statistical significance was defined as $P < 0.05$.

Acknowledgements

We thank Fidel Albornoz (Facultad Ciencias Químicas y Farmacéuticas, Universidad de Chile, Sergio Livingstone P 1007, Santiago, Chile) for his excellent technical assistance.

Competing interests

The authors declare no competing interests.

Author contributions

C.P. carried out project design and all experiments, except those stated separately, and wrote the manuscript; V.P. helped with project design, manuscript writing and carried out the oxygen consumption determinations and cytosolic Ca^{2+} determinations; C.L.C. performed the confocal microscopy experiments with prazosin; P.M. helped with mitochondrial morphological analysis; A. de C. helped with β -MHC western blots and data discussion; T.G. helped with adenoviral phalloidin-Rhodamine experiments; P.R.M. performed the RCAN 1.4 western blots; R.Z. helped with mitochondrial mass measurements; J.K. helped with calcineurin-related adenovirus imaging analysis and mitochondrial isolation experiments; M.C. guided the adenovirus purification, experiments with these tools and helped with figure preparation; A.Z. provided the AsMfn2 and DrpK38A adenovirus; B.A.R. planned and supervised all the experiments related to calcineurin pathway and mitophagy, discussed the data and edited the final manuscript; and S.L. conceived and supervised the whole project, discussed the data and edited the final manuscript.

Funding

This work was supported by Fondo Nacional de Desarrollo Científico y Tecnológico (FONDECYT) [grant number 1120212 to S.L.]; Comisión Nacional de Investigación Científica y tecnológica (CONICYT) [grant numbers Anillo ACT 1111 to S.L. and M.C., Redes 120003 to S.L., FONDAPE 15130011 to S.L.]; the Ministerio de Educación y Ciencia (MEC) [grant number SAF2008-03803 to A.Z.]; the Generalitat de Catalunya, CIBERDEM, Instituto de Salud Carlos III [grant number 2009SGR915 to A.Z.]; and the National Institutes of Health [grant numbers HL-072016, HL-097768 to B.A.R.]. We are thankful for the PhD or MSc fellowships from CONICYT, Chile to C.P., V.P., C.L.C., P.E.M., A. de C., J.K. and R.Z. C.P. holds a CONICYT post-doctoral scholarship (3130749), CONICYT, Chile. We thank Becas, Chile, and the American Heart Association for the postdoctoral funding to V.P. Deposited in PMC for release after 12 months.

Supplementary material

Supplementary material available online at <http://jcs.biologists.org/lookup/suppl/doi:10.1242/jcs.139394/-DC1>

References

- Ahuja, P., Sdek, P. and MacLellan, W. R. (2007). Cardiac myocyte cell cycle control in development, disease, and regeneration. *Physiol. Rev.* **87**, 521–544.
- Ashrafian, H., Docherty, L., Leo, V., Towilson, C., Neilan, M., Steeples, V., Lygate, C. A., Hough, T., Townsend, S., Williams, D. et al. (2010). A mutation in the mitochondrial fission gene Dnm1l leads to cardiomyopathy. *PLoS Genet.* **6**, e1001000.

- Bach, D., Pich, S., Soriano, F. X., Vega, N., Baumgartner, B., Oriola, J., Daugaard, J. R., Lloberas, J., Camps, M., Zierath, J. R. et al. (2003). Mitofusin-2 determines mitochondrial network architecture and mitochondrial metabolism. A novel regulatory mechanism altered in obesity. *J. Biol. Chem.* **278**, 17190–17197.
- Barki-Harrington, L., Perrino, C. and Rockman, H. A. (2004). Network integration of the adrenergic system in cardiac hypertrophy. *Cardiovasc. Res.* **63**, 391–402.
- Barry, S. P., Davidson, S. M. and Townsend, P. A. (2008). Molecular regulation of cardiac hypertrophy. *Int. J. Biochem. Cell Biol.* **40**, 2023–2039.
- Benard, G., Bellance, N., James, D., Parrone, P., Fernandez, H., Letellier, T. and Rossignol, R. (2007). Mitochondrial bioenergetics and structural network organization. *J. Cell Sci.* **120**, 838–848.
- Beraud, N., Pelloux, S., Usson, Y., Kuznetsov, A. V., Ronot, X., Tourneur, Y. and Saks, V. (2009). Mitochondrial dynamics in heart cells: very low amplitude high frequency fluctuations in adult cardiomyocytes and flow motion in non beating HL-1 cells. *J. Bioenerg. Biomembr.* **41**, 195–214.
- Bereiter-Hahn, J. and Vöth, M. (1994). Dynamics of mitochondria in living cells: shape changes, dislocations, fusion, and fission of mitochondria. *Microsc. Res. Tech.* **27**, 198–219.
- Bernardo, B. C., Weeks, K. L., Pretorius, L. and McMullen, J. R. (2010). Molecular distinction between physiological and pathological cardiac hypertrophy: experimental findings and therapeutic strategies. *Pharmacol. Ther.* **128**, 191–227.
- Bravo, R., Parra, V., Gatica, D., Rodríguez, A. E., Torrealba, N., Paredes, F., Wang, Z. V., Zorzano, A., Hill, J. A., Jaimovich, E. et al. (2013). Endoplasmic reticulum and the unfolded protein response: dynamics and metabolic integration. *Int. Rev. Cell Mol. Biol.* **301**, 215–290.
- Buchwald, A., Till, H., Unterberg, C., Oberschmidt, R., Figulla, H. R. and Wiegand, V. (1990). Alterations of the mitochondrial respiratory chain in human dilated cardiomyopathy. *Eur. Heart J.* **11**, 509–516.
- Bueno, O. F., De Windt, L. J., Tymitz, K. M., Witt, S. A., Kimball, T. R., Klevitsky, R., Hewett, T. E., Jones, S. P., Lefer, D. J., Peng, C. F. et al. (2000). The MEK1-ERK1/2 signaling pathway promotes compensated cardiac hypertrophy in transgenic mice. *EMBO J.* **19**, 6341–6350.
- Cárdenas, C., Miller, R. A., Smith, I., Bui, T., Molgó, J., Müller, M., Vais, H., Cheung, K. H., Yang, J., Parker, I. et al. (2010). Essential regulation of cell bioenergetics by constitutive InsP3 receptor Ca²⁺ transfer to mitochondria. *Cell* **142**, 270–283.
- Cereghetti, G. M., Stangherlin, A., Martins de Brito, O., Chang, C. R., Blackstone, C., Bernardi, P. and Scorrano, L. (2008). Dephosphorylation by calcineurin regulates translocation of Drp1 to mitochondria. *Proc. Natl. Acad. Sci. USA* **105**, 15803–15808.
- Chan, D. C. (2006). Dissecting mitochondrial fusion. *Dev. Cell* **11**, 592–594.
- Chan, C. R. and Blackstone, C. (2007). Cyclic AMP-dependent protein kinase phosphorylation of Drp1 regulates its GTPase activity and mitochondrial morphology. *J. Biol. Chem.* **282**, 21583–21587.
- Chen, Y. and Dorn, G. W., I. I. (2013). PINK1-phosphorylated mitofusin 2 is a Parkin receptor for culling damaged mitochondria. *Science* **340**, 471–475.
- Chen, H., Detmer, S. A., Ewald, A. J., Griffin, E. E., Fraser, S. E. and Chan, D. C. (2003). Mitofusins Mfn1 and Mfn2 coordinately regulate mitochondrial fusion and are essential for embryonic development. *J. Cell Biol.* **160**, 189–200.
- Chen, H., Chomyn, A. and Chan, D. C. (2005). Disruption of fusion results in mitochondrial heterogeneity and dysfunction. *J. Biol. Chem.* **280**, 26185–26192.
- Chen, L., Gong, Q., Stice, J. P. and Knowlton, A. A. (2009). Mitochondrial OPA1, apoptosis, and heart failure. *Cardiovasc. Res.* **84**, 91–99.
- Chiong, M., Parra, V., Eisner, V., Ibarra, C., Maldonado, C., Criollo, A., Bravo, R., Quiroga, C., Contreras, A., Vicencio, J. M. et al. (2010). Parallel activation of Ca²⁺-induced survival and death pathways in cardiomyocytes by sorbitol-induced hyperosmotic stress. *Apoptosis* **15**, 887–903.
- Clerk, A., Aggeli, I. K., Stathopoulou, K. and Sugden, P. H. (2006). Peptide growth factors signal differentially through protein kinase C to extracellular signal-regulated kinases in neonatal cardiomyocytes. *Cell. Signal.* **18**, 225–235.
- Costes, S. V., Daelemans, D., Cho, E. H., Dobbin, Z., Pavlakis, G. and Lockett, S. (2004). Automatic and quantitative measurement of protein-protein colocalization in live cells. *Biophys. J.* **86**, 3993–4003.
- Cribbs, J. T. and Strack, S. (2007). Reversible phosphorylation of Drp1 by cyclic AMP-dependent protein kinase and calcineurin regulates mitochondrial fission and cell death. *EMBO Rep.* **8**, 939–944.
- Criollo, A., Galluzzi, L., Maiuri, M. C., Tasdemir, E., Lavandro, S. and Kroemer, G. (2007). Mitochondrial control of cell death induced by hyperosmotic stress. *Apoptosis* **12**, 3–18.
- Day, H. E., Campeau, S., Watson, S. J., Jr and Akil, H. (1997). Distribution of alpha 1a-, alpha 1b- and alpha 1d-adrenergic receptor mRNA in the rat brain and spinal cord. *J. Chem. Neuroanat.* **13**, 115–139.
- de Brito, O. M. and Scorrano, L. (2008). Mitofusin 2 tethers endoplasmic reticulum to mitochondria. *Nature* **456**, 605–610.
- de Brito, O. M. and Scorrano, L. (2009). Mitofusin-2 regulates mitochondrial and endoplasmic reticulum morphology and tethering: the role of Ras. *Mitochondrion* **9**, 222–226.
- del Campo, A., Parra, V., Vázquez-Trincado, C., Gutiérrez, T., Morales, P. E., López-Crisosto, C., Bravo-Sagua, R., Navarro-Marquez, M. F., Verdejo, H. E., Contreras-Ferrat, A. et al. (2014). Mitochondrial fragmentation impairs insulin-dependent glucose uptake by modulating Akt activity through mitochondrial Ca²⁺ uptake. *Am. J. Physiol.* **306**, E1–E13.
- Delling, U., Tureckova, J., Lim, H. W., De Windt, L. J., Rotwein, P. and Molkenin, J. D. (2000). A calcineurin-NFATc3-dependent pathway regulates skeletal muscle differentiation and slow myosin heavy-chain expression. *Mol. Cell. Biol.* **20**, 6600–6611.
- Diwan, A. and Dorn, G. W., I. I. (2007). Decompensation of cardiac hypertrophy: cellular mechanisms and novel therapeutic targets. *Physiology (Bethesda)* **22**, 56–64.
- Ehres, S., Raschke, I., Mancuso, G., Bernacchia, A., Geimer, S., Tondera, D., Martinou, J. C., Westermann, B., Rugaril, E. I. and Langer, T. (2009). Regulation of OPA1 processing and mitochondrial fusion by m-AAA protease isoenzymes and OMA1. *J. Cell Biol.* **187**, 1023–1036.
- Fang, L., Moore, X. L., Gao, X. M., Dart, A. M., Lim, Y. L. and Du, X. J. (2007). Down-regulation of mitofusin-2 expression in cardiac hypertrophy in vitro and in vivo. *Life Sci.* **80**, 2154–2160.
- Frey, N., Katus, H. A., Olson, E. N. and Hill, J. A. (2004). Hypertrophy of the heart: a new therapeutic target? *Circulation* **109**, 1580–1589.
- Galvez, A., Morales, M. P., Eltit, J. M., Ocaranza, P., Carrasco, L., Campos, X., Sapag-Hagar, M., Diaz-Araya, G. and Lavandro, S. (2001). A rapid and strong apoptotic process is triggered by hyperosmotic stress in cultured rat cardiac myocytes. *Cell Tissue Res.* **304**, 279–285.
- Gandre-Babbe, S. and van der Bliek, A. M. (2008). The novel tail-anchored membrane protein Mff controls mitochondrial and peroxisomal fission in mammalian cells. *Mol. Biol. Cell* **19**, 2402–2412.
- Givvimani, S., Munjal, C., Tyagi, N., Sen, U., Metreveli, N. and Tyagi, S. C. (2012). Mitochondrial division/mitophagy inhibitor (Mdivi) ameliorates pressure overload induced heart failure. *PLoS ONE* **7**, e32388.
- Graham, B. H., Waymire, K. G., Cottrell, B., Trowace, I. A., MacGregor, G. R. and Wallace, D. C. (1997). A mouse model for mitochondrial myopathy and cardiomyopathy resulting from a deficiency in the heart/muscle isoform of the adenine nucleotide translocator. *Nat. Genet.* **16**, 226–234.
- Head, B., Griparic, L., Amiri, M., Gandre-Babbe, S. and van der Bliek, A. M. (2009). Inducible proteolytic inactivation of OPA1 mediated by the OMA1 protease in mammalian cells. *J. Cell Biol.* **187**, 959–966.
- Heineke, J. and Molkenin, J. D. (2006). Regulation of cardiac hypertrophy by intracellular signalling pathways. *Nat. Rev. Mol. Cell Biol.* **7**, 589–600.
- Hernández-Alvarez, M. I., Paz, J. C., Sebastián, D., Muñoz, J. P., Liesa, M., Segalés, J., Palacin, M. and Zorzano, A. (2013). Glucocorticoid modulation of mitochondrial function in hepatoma cells requires the mitochondrial fission protein Drp1. *Antioxid. Redox Signal.* **19**, 366–378.
- Huss, J. M. and Kelly, D. P. (2005). Mitochondrial energy metabolism in heart failure: a question of balance. *J. Clin. Invest.* **115**, 547–555.
- Ibarra, C., Estrada, M., Carrasco, L., Chiong, M., Liberona, J. L., Cardenas, C., Diaz-Araya, G., Jaimovich, E. and Lavandro, S. (2004). Insulin-like growth factor-1 induces an inositol 1,4,5-trisphosphate-dependent increase in nuclear and cytosolic calcium in cultured rat cardiac myocytes. *J. Biol. Chem.* **279**, 7554–7565.
- Ishihara, N., Fujita, Y., Oka, T. and Mihara, K. (2006). Regulation of mitochondrial morphology through proteolytic cleavage of OPA1. *EMBO J.* **25**, 2966–2977.
- Javadov, S., Rajapurohitam, V., Kilić, A., Hunter, J. C., Zeidan, A., Said Faruq, N., Escobales, N. and Karmazyn, M. (2011). Expression of mitochondrial fusion-fission proteins during post-infarction remodeling: the effect of NHE-1 inhibition. *Basic Res. Cardiol.* **106**, 99–109.
- Jofuku, A., Ishihara, N. and Mihara, K. (2005). Analysis of functional domains of rat mitochondrial Fis1, the mitochondrial fission-stimulating protein. *Biochem. Biophys. Res. Commun.* **333**, 650–659.
- Kanzaki, Y., Terasaki, F., Okabe, M., Otsuka, K., Katashima, T., Fujita, S., Ito, T. and Kitaura, Y. (2010). Giant mitochondria in the myocardium of a patient with mitochondrial cardiomyopathy: transmission and 3-dimensional scanning electron microscopy. *Circulation* **121**, 831–832.
- Kuzmicki, J., Del Campo, A., López-Crisosto, C., Morales, P. E., Penanen, C., Bravo-Sagua, R., Hechenleitner, J., Zepeda, R., Castro, P. F., Verdejo, H. E. et al. (2011). [Mitochondrial dynamics: a potential new therapeutic target for heart failure]. *Rev. Esp. Cardiol.* **64**, 916–923.
- Liesa, M., Borda-d'Agua, B., Medina-Gómez, G., Lelliott, C. J., Paz, J. C., Rojo, M., Palacin, M., Vidal-Puig, A. and Zorzano, A. (2008). Mitochondrial fusion is increased by the nuclear coactivator PGC-1beta. *PLoS ONE* **3**, e3613.
- Liu, Q., D'Silva, P., Walter, W., Marszalek, J. and Craig, E. A. (2003). Regulated cycling of mitochondrial Hsp70 at the protein import channel. *Science* **300**, 139–141.
- Manders, E. M. M., Verbeek, F. J. and Aten, J. A. (1993). Measurement of colocalization of objects in dual-color confocal images. *J. Microsc.* **169**, 375–382.
- Marambaio, P., Toro, B., Sanhueza, C., Troncoso, R., Parra, V., Verdejo, H., García, L., Quiroga, C., Munafó, D., Diaz-Elizondo, J. et al. (2010). Glucose deprivation causes oxidative stress and stimulates aggresome formation and autophagy in cultured cardiac myocytes. *Biochim. Biophys. Acta* **1802**, 509–518.
- Marian, A. J. and Roberts, R. (1995). Recent advances in the molecular genetics of hypertrophic cardiomyopathy. *Circulation* **92**, 1336–1347.
- Molkenin, J. D., Lu, J. R., Antos, C. L., Markham, B., Richardson, J., Robbins, J., Grant, S. R. and Olson, E. N. (1998). A calcineurin-dependent transcriptional pathway for cardiac hypertrophy. *Cell* **93**, 215–228.

- Munoz, J. P., Chiong, M., García, L., Troncoso, R., Toro, B., Pedrozo, Z., Diaz-Elizondo, J., Salas, D., Parra, V., Núñez, M. T. et al. (2010). Iron induces protection and necrosis in cultured cardiomyocytes: Role of reactive oxygen species and nitric oxide. *Free Radic. Biol. Med.* **48**, 526–534.
- Neubauer, S. (2007). The failing heart – an engine out of fuel. *N. Engl. J. Med.* **356**, 1140–1151.
- Okamoto, K. and Shaw, J. M. (2005). Mitochondrial morphology and dynamics in yeast and multicellular eukaryotes. *Annu. Rev. Genet.* **39**, 503–536.
- Ong, S. B., Subrayan, S., Lim, S. Y., Yellon, D. M., Davidson, S. M. and Hausenloy, D. J. (2010). Inhibiting mitochondrial fission protects the heart against ischemia/reperfusion injury. *Circulation* **121**, 2012–2022.
- Otera, H., Wang, C., Cleland, M. M., Setoguchi, K., Yokota, S., Youle, R. J. and Mihara, K. (2010). Mif is an essential factor for mitochondrial recruitment of Drp1 during mitochondrial fission in mammalian cells. *J. Cell Biol.* **191**, 1141–1158.
- Papanicolaou, K. N., Khairallah, R. J., Ngoh, G. A., Chikando, A., Luptak, I., O’Shea, K. M., Riley, D. D., Lugus, J. J., Colucci, W. S., Lederer, W. J. et al. (2011). Mitofusin-2 maintains mitochondrial structure and contributes to stress-induced permeability transition in cardiac myocytes. *Mol. Cell. Biol.* **31**, 1309–1328.
- Parone, P. A., Da Cruz, S., Tondera, D., Mattenberger, Y., James, D. I., Maechler, P., Barja, F. and Martinou, J. C. (2008). Preventing mitochondrial fission impairs mitochondrial function and leads to loss of mitochondrial DNA. *PLoS ONE* **3**, e3257.
- Parra, V., Eisner, V., Chiong, M., Criollo, A., Moraga, F., García, A., Härtel, S., Jaimovich, E., Zorzano, A., Hidalgo, C. et al. (2008). Changes in mitochondrial dynamics during ceramide-induced cardiomyocyte early apoptosis. *Cardiovasc. Res.* **77**, 387–397.
- Parra, V., Verdejo, H. E., Iglewski, M., Del Campo, A., Troncoso, R., Jones, D., Zhu, Y., Kuzmicic, J., Pennanen, C., Lopez-Crisosto, C. et al. (2014). Insulin stimulates mitochondrial fusion and function in cardiomyocytes via the Akt-mTOR-NF κ B-Opa-1 signaling pathway. *Diabetes* **63**, 75–88.
- Perlini, S., Ferrero, I., Palladini, G., Tozzi, R., Gatti, C., Vezzoli, M., Cesana, F., Janetti, M. B., Clari, F., Busca, G. et al. (2006). Survival benefits of different antiadrenergic interventions in pressure overload left ventricular hypertrophy/failure. *Hypertension* **48**, 93–97.
- Pich, S., Bach, D., Briones, P., Liesa, M., Camps, M., Testar, X., Palacín, M. and Zorzano, A. (2005). The Charcot-Marie-Tooth type 2A gene product, Mfn2, up-regulates fuel oxidation through expression of OXPHOS system. *Hum. Mol. Genet.* **14**, 1405–1415.
- Ramirez, M. T., Sah, V. P., Zhao, X. L., Hunter, J. J., Chien, K. R. and Brown, J. H. (1997). The MEKK-JNK pathway is stimulated by alpha1-adrenergic receptor and ras activation and is associated with in vitro and in vivo cardiac hypertrophy. *J. Biol. Chem.* **272**, 14057–14061.
- Ramírez, O., García, A., Rojas, R., Couve, A. and Härtel, S. (2010). Confined displacement algorithm determines true and random colocalization in fluorescence microscopy. *J. Microsc.* **239**, 173–183.
- Rothermel, B. A., Vega, R. B. and Williams, R. S. (2003). The role of modulatory calcineurin-interacting proteins in calcineurin signaling. *Trends Cardiovasc. Med.* **13**, 15–21.
- Ruwhof, C. and van der Laarse, A. (2000). Mechanical stress-induced cardiac hypertrophy: mechanisms and signal transduction pathways. *Cardiovasc. Res.* **47**, 23–37.
- Santel, A. and Frank, S. (2008). Shaping mitochondria: The complex posttranslational regulation of the mitochondrial fission protein DRP1. *IUBMB Life* **60**, 448–455.
- Shibasaki, F., Hallin, U. and Uchino, H. (2002). Calcineurin as a multifunctional regulator. *J. Biochem.* **131**, 1–15.
- Smirnova, E., Griparic, L., Shurland, D. L. and van der Bliek, A. M. (2001). Dynamin-related protein Drp1 is required for mitochondrial division in mammalian cells. *Mol. Biol. Cell* **12**, 2245–2256.
- Song, Z., Chen, H., Fiket, M., Alexander, C. and Chan, D. C. (2007). OPA1 processing controls mitochondrial fusion and is regulated by mRNA splicing, membrane potential, and Yme1L. *J. Cell Biol.* **178**, 749–755.
- Song, Z., Ghochani, M., McCaffery, J. M., Frey, T. G. and Chan, D. C. (2009). Mitofusins and OPA1 mediate sequential steps in mitochondrial membrane fusion. *Mol. Biol. Cell* **20**, 3525–3532.
- Stojanovski, D., Koutsopoulos, O. S., Okamoto, K. and Ryan, M. T. (2004). Levels of human Fis1 at the mitochondrial outer membrane regulate mitochondrial morphology. *J. Cell Sci.* **117**, 1201–1210.
- Szabadkai, G., Simoni, A. M., Chami, M., Wieckowski, M. R., Youle, R. J. and Rizzuto, R. (2004). Drp-1-dependent division of the mitochondrial network blocks intraorganellar Ca²⁺ waves and protects against Ca²⁺-mediated apoptosis. *Mol. Cell* **16**, 59–68.
- Taigen, T., De Windt, L. J., Lim, H. W. and Molkenkin, J. D. (2000). Targeted inhibition of calcineurin prevents agonist-induced cardiomyocyte hypertrophy. *Proc. Natl. Acad. Sci. USA* **97**, 1196–1201.
- Twig, G., Elorza, A., Molina, A. J., Mohamed, H., Wikstrom, J. D., Walzer, G., Stiles, L., Haigh, S. E., Katz, S., Las, G. et al. (2008). Fission and selective fusion govern mitochondrial segregation and elimination by autophagy. *EMBO J.* **27**, 433–446.
- Vendelin, M., Béraud, N., Guerrero, K., Andrienko, T., Kuznetsov, A. V., Olivares, J., Kay, L. and Saks, V. A. (2005). Mitochondrial regular arrangement in muscle cells: a “crystal-like” pattern. *Am. J. Physiol.* **288**, C757–C767.
- Wang, J. X., Jiao, J. Q., Li, Q., Long, B., Wang, K., Liu, J. P., Li, Y. R. and Li, P. F. (2011). miR-499 regulates mitochondrial dynamics by targeting calcineurin and dynamin-related protein-1. *Nat. Med.* **17**, 71–78.
- Wilkins, B. J. and Molkenkin, J. D. (2004). Calcium-calcineurin signaling in the regulation of cardiac hypertrophy. *Biochem. Biophys. Res. Commun.* **322**, 1178–1191.
- Yoon, Y., Krueger, E. W., Oswald, B. J. and McNiven, M. A. (2003). The mitochondrial protein hFis1 regulates mitochondrial fission in mammalian cells through an interaction with the dynamin-like protein DLP1. *Mol. Cell. Biol.* **23**, 5409–5420.
- Yu, T., Robotham, J. L. and Yoon, Y. (2006). Increased production of reactive oxygen species in hyperglycemic conditions requires dynamic change of mitochondrial morphology. *Proc. Natl. Acad. Sci. USA* **103**, 2653–2658.
- Yu, H., Guo, Y., Mi, L., Wang, X., Li, L. and Gao, W. (2011). Mitofusin 2 inhibits angiotensin II-induced myocardial hypertrophy. *J. Cardiovasc. Pharmacol. Ther.* **16**, 205–211.